

First-principles study of small-radius single-walled BN nanotubes

H.J. Xiang, Jinlong Yang,* J.G. Hou, and Qingshi Zhu

Laboratory of Bond Selective Chemistry and Structure Research Laboratory, University of Science and Technology of China, Hefei, Anhui 230026, People's Republic of China

(Received 10 January 2003; revised manuscript received 4 April 2003; published 30 July 2003)

The structural, electronic, and vibrational properties of small-radius single-walled BN nanotubes are studied using the density functional method with the local density approximation. The results show that the chirality preference of BN nanotubes observed in experiments may be explained from the relative stability of the corresponding BN strips. Compared with the armchair BN strips, the zigzag BN strips have larger binding energies and thus may be more easily formed. The smallest stable BN nanotube is found to be the (5,0) zigzag nanotube. The energy gap of small zigzag BN nanotubes decreases rapidly with the decrease of radius. The phonon dispersions of BN nanotubes are calculated and the frequency of the radial breathing mode is found to be inversely proportional to the nanotube radius.

DOI: 10.1103/PhysRevB.68.035427

PACS number(s): 61.46.+w, 73.22.-f, 63.22.+m

I. INTRODUCTION

BN nanotubes^{1,2} are a kind of tubular material combining ultimate strength and stable dielectric properties. They are predicted to be semiconductors regardless of diameter, chirality, or the number of walls of the tube.^{1,3} This contrasts markedly with the heterogeneity of electronic properties of carbon nanotubes, and also makes pure BN nanotubes particularly useful for potential device applications. It has already been realized that BN tubes have several unmatched structural features which have never been noticed for C and other inorganic compound tubes.⁴ One of these features is that BN nanotubes have a chirality preference, that is, the tube axes “prefer” the 1010 direction of the graphenelike sheet (so-called zigzag tubes).⁵ Before this feature was discovered experimentally, Blase *et al.*⁶ gave a contrary theoretical prediction that the growth of single-walled armchair BN nanotubes would be better favored than the zigzag ones based on the *ab initio* molecular dynamics simulations. Afterward, Menon *et al.*⁷ related the observed feature to the effect of relaxation on the chirality of nanotubes based on the structural data obtained by the generalized tight-binding molecular dynamics method, but they did not confirm their analysis from an energy point of view. Obviously, further theoretical investigations are required to rationalize the experimental observation.

The stability of nanotubes has been an important issue in nanotube researches. Carbon nanotubes with diameters of about 0.4 nm have been proved to be the smallest stable ones experimentally⁸ and theoretically.⁹ For BN nanotubes, however, there has been no study on this problem. How small the BN nanotube can be is still an open question.

Vibrational spectroscopy has been one of useful tools to characterize carbon nanotube samples. There are many experimental and theoretical studies on the vibrational properties of carbon nanotubes. Especially, the Raman-active radial breathing mode (RBM) is found to be inversely proportional to the radius of a carbon nanotube, and offers a rapid way of estimating the diameter distribution of tubes present in a sample.^{10,11} However, similar studies on BN nanotubes are very few. Very recently, Sánchez-Portal and Hernández reported a semiempirical tight-binding study on the vibrational

properties of BN single-walled nanotubes.¹²

In this paper, we perform a systematic first-principles study on small-radius single-walled BN nanotubes. The chirality preference, smallest nanotube, and the RBM of BN nanotubes are investigated. We describe our computational method in Sec. II, and present our results and discussions in Sec. III. Finally, a summary is given in Sec. IV.

II. COMPUTATIONAL METHOD

Our calculations are performed using the Vienna *ab initio* simulation package (VASP).^{13,14} In VASP, the generalized self-consistent Kohn-Sham equations are solved using an efficient matrix-diagonalization routine based on a sequential band-by-band residual minimization method and a Pulay-like charge density mixing.^{15,16} The electron-ion interaction is described by ultrasoft Vanderbilt-type pseudopotentials,¹⁷ allowing for a low cutoff energy in the plane-wave expansion of the valence states. The cutoff energy is set to 347.9 eV in the present work. The conjugate gradient method is employed to optimize the geometry until all the forces are small than 0.01 eV/Å. All calculations are performed using the local density approximation (LDA) in the density functional theory (DFT).^{18,19} For the exchange-correlation energy among electrons, we use a functional form²⁰ fitted to the Monte Carlo results for the homogeneous electron gas.²¹ Although VASP always employs periodic boundary conditions, our calculations for BN single-walled nanotubes relate to infinitely long isolated tubes. This is achieved by arranging the tubes in a hexagonal lattice with lattice parameters of 20 Å in the directions perpendicular to the tube axis, and only parallel to the tube axis (*z* direction) the periodicity is maintained. The resulting vacuum region is so large that there is almost no interaction between the tubes. To verify this point, we have done two phonon calculations for a BN(5,0) nanotube with lattice parameters of 22.3 and 17.78 Å respectively. The difference of the same phonon mode between the two calculations is less than 6 cm⁻¹. BN plane strips are treated in the same way. Five irreducible *k* points are used in the *z* direction to calculate the total energy and the forces of the nanotubes accurately. Six and seven irreducible *k* points are used for zigzag strips and armchair strips respectively.

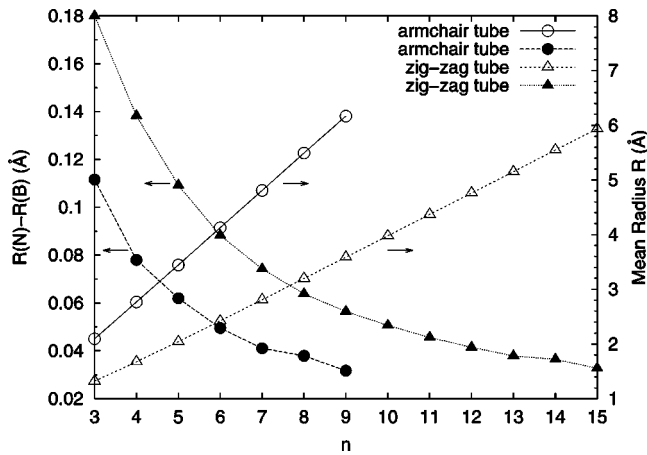


FIG. 1. The mean radii and separations between the two cylinders of the optimized BN nanotubes.

III. RESULTS AND DISCUSSION

We have optimized the zigzag $(n,0)$ nanotube with $n = 3-15$ and the armchair (n,n) nanotube with $n = 3-9$ BN nanotubes. In our optimized nanotubes, the boron atoms rotate inward to an approximately planar configuration, whereas nitrogen atoms move outward into another planar configuration. This buckling results in two cylinders formed by boron atoms and nitrogen atoms respectively. Figure 1 shows the mean radii and separations between the two cylinders of the optimized BN nanotubes. From Fig. 1, one can find that the smaller the nanotube is, the bigger the separation between the two cylinders is. For example, the separation is 0.11 and 0.03 Å for BN(5,0) and BN(15,0) respectively. Our results agree qualitatively with those obtained by Blase *et al.*³ and by Kudin *et al.*²² In their studies, they used DFT with the pseudopotential plane wave basis set and with the Gaussian type 3-21G basis set respectively.

The total energies of BN nanotubes and an isolated BN plane sheet are displayed in Fig. 2. The strain energy of a BN nanotube can be defined as the energy difference between the

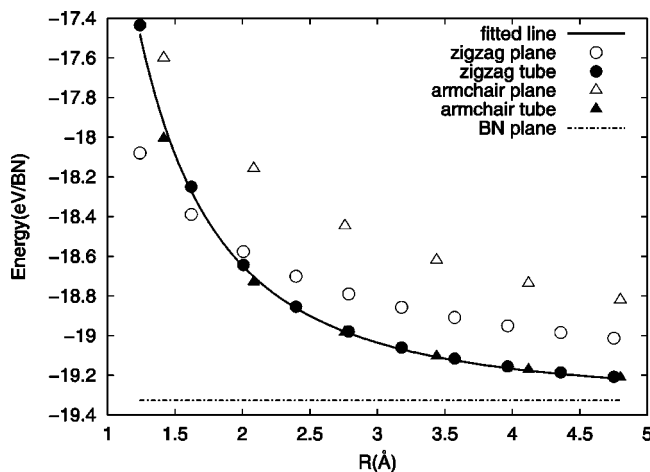


FIG. 2. The total energies of BN nanotubes, BN strips, and an isolated BN plane sheet. The radius refers to that of an unrelaxed BN nanotube.

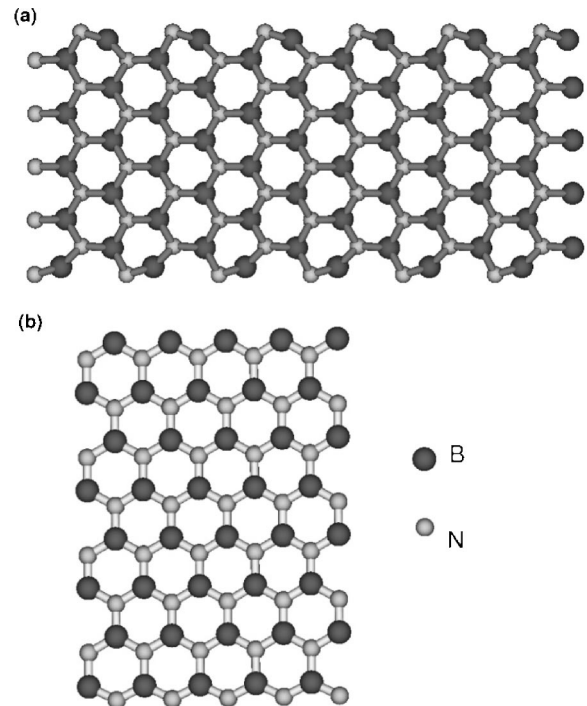


FIG. 3. Relaxed structures of (a) a BN(5,0) strip, and (b) a BN(4,4) strip.

BN nanotube and plane sheet. From this figure, we can find that the strain energy of a BN nanotube depends only on its radius, but not on its chirality, contrasting sharply with the suggestion of Menon *et al.*⁷ In fact, we can use a formula $E_{strain} = 2.89938/R^{2.09481}$ to fit the strain energy of a BN nanotube, where the units of energy and radius are eV and Å respectively. This formula is consistent with the conventional elastic theorem. Our fitting results agree well with those from non-orthogonal tight-binding calculations by Hernández *et al.*,^{23,24} who gave a behavior of $2.839/R^{1.984}$ for BN($n,0$) tubes and $2.781/R^{1.980}$ for BN(n,n) tubes respectively. The calculations of Kudin *et al.*²² gave a behavior of $3.30/R^2$, and the discrepancy between theirs and ours may be due to different exchange-correlation functionals and basis sets used in calculations.

Since BN nanotubes can be viewed as formed by rolling the h-BN sheet, we have studied the corresponding BN strips. First we optimize the structures of BN strips. Figure 3 shows the relaxed structures of two typical zigzag and armchair strips. While the structural relaxation for armchair BN strips is rather small, that for zigzag strips is very distinct. The unsaturated B-N dimers at the two sides of zigzag strips are buckled greatly. This kind of structural relaxation lowers the energy of system, as shown in Fig. 2. As a result, the zigzag BN strips are more stable than armchair strips with similar widths. Thus we can propose a growth process of BN nanotubes to understand the chirality preference observed in experiments: first the BN zigzag strips are formed because of their favorable energies; then the BN zigzag nanotubes are formed from the BN zigzag strips. Experimentally, the chirality preferential growths are observed in BN nanotubes produced by laser heating at high pressure or by thermo-

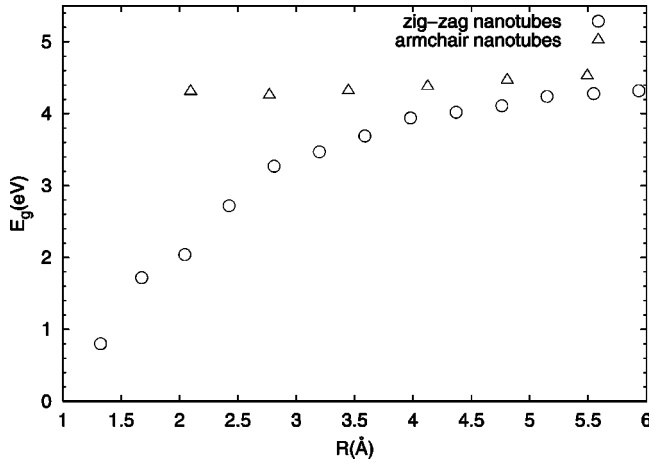


FIG. 4. Energy gaps of $\text{BN}(n,0)$ zigzag nanotubes with $n=3-15$ and $\text{BN}(n,n)$ armchair nanotubes with $n=3-8$. The radius refers to that of an unrelaxed BN nanotube.

chemical processes. At these growth conditions, the h-BN particles or sheets could pre-exist. In addition, we find that the carbon zigzag strips do not take such a kind of structural relaxation, and the energy difference between the zigzag and armchair carbon strips with similar widths is small. These results indicate that the growth of carbon nanotubes is not the chirality preference, in good agreement with the experimental observation.

With the total energies of BN nanotubes and strips at hand, we now can address the problem of the smallest stable BN nanotube. In Fig. 2, we can see there is a crossover between the energy curve of zigzag strips and that of zigzag nanotubes. For $n \geq 5$, $(n,0)$ zigzag nanotubes are more stable than zigzag strips, but for $n < 5$ the relationship is reversed. So, from the energy point of view, the smallest stable BN nanotube will be a $(5,0)$ zigzag nanotube, which has a radius of about 2.0 Å.

Though it is a generally view that BN nanotubes are semiconductors with a nearly constant quasiparticle energy gap of 5.5 eV regardless of diameter, chirality, or the number of walls of the tube,³ very small nanotubes are expected to have some different energy gap dependences because of the strong hybridization effect. Here we have calculated the electronic structure of the zigzag $(n,0)$ (with $n=3-15$) and armchair (n,n) (with $n=3-8$ BN) nanotubes. We show the calculated energy gap results in Fig. 4. From the figure, one can find that the energy gap of small zigzag BN nanotubes decreases rapidly with a decrease of the radius, while that for armchair nanotubes changes a little. This different behavior has been explained by Blase *et al.*³ They showed that for armchair tubes the near free electronic state at Γ corresponds to the bottom of the conducting band while this is not the case for zigzag nanotube. We also find that all the small zigzag nanotubes are direct gap semiconductors and all the armchair nanotubes are indirect gap semiconductors, consistent with previous theoretical results.³ It is well known that the LDA calculation underestimates the energy gap. Since the quasiparticle energy gap of large BN single-walled nanotubes is 5.5 eV (Ref. 3) and our LDA gap of $\text{BN}(15,0)$ is 4.3 eV, we estimate the quasiparticle correction of the LDA energy gap

is 1.2 eV for $\text{BN}(15,0)$. If we assume this correction can apply for the smaller BN nanotubes, we will have a quasiparticle energy gap of 3.2 eV for $\text{BN}(5,0)$ which approaches the energy gap of GaN. So $\text{BN}(5,0)$ may be used as quasi-1D optoelectronic device.

We use a direct approach²⁵ to study the phonon properties of BN single-walled nanotubes. Within the harmonic approximation, the phonon frequencies and phonon modes are obtained by diagonalizing the dynamical matrix given at each wave vector by

$$D_{\alpha\beta}^{i,j} = \frac{1}{\sqrt{M_i M_j}} \sum_{\mathbf{R}} \exp\{i\mathbf{k} \cdot (\tau_i - \tau_j - \mathbf{R})\} \Phi_{\alpha\beta}^{i,j}(\tau_i - \tau_j - \mathbf{R}),$$

where $\Phi_{\alpha\beta}^{i,j}(\tau_i - \tau_j - \mathbf{R})$, \mathbf{R} , M_i and τ_i are the force constants, lattice vectors, mass, and position of each atom in the unit cell respectively. Labels i and j denote the atoms in the unit cell, while α and β denote the Cartesian coordinates (x, y, z) of the atomic displacement.

In order to calculate the force constants, $1 \times 1 \times 3$ supercell is used for BN nanotubes. In general, we need to perform $6N$ times supercell total-energy calculations because each atom in the unit cell needs two displacements in all three directions (N is the number of atoms in the unit cell of the system). But because of the symmetry of BN nanotubes, there are only two kinds of ions, so we can reduce the displacement number to 12 for all kinds of BN nanotubes. The other force constants can be obtained using symmetry. To check the accuracy of our method, we calculate the phonon band structure of h-BN plane sheet first. In this calculation, we use a $3 \times 3 \times 1$ supercell containing 18 atoms. The calculated frequency of the Raman-active E_{2g} mode due to B and N atoms moving against each other in a plane is 1379 cm^{-1} , which is very close to the experimental value 1366 cm^{-1} .²⁶ This result also agrees well with that of Ohba *et al.*²⁷ using density-functional perturbation theory (1382 cm^{-1}) and that of Kern *et al.*²⁸ using *ab initio* force constant method (1390 cm^{-1}).

We show the phonon DOS and phonon band structure of $\text{BN}(5,0)$ in Fig. 5. The phonon DOS of the $\text{BN}(5,0)$ nanotube is similar to that of the h-BN plane sheet, except for more complicated structures. Moreover, the nanotube has a constant phonon DOS in low frequency ($0 < \nu < 100 \text{ cm}^{-1}$) which is the character of phonon DOS of one-dimensional or quasi-one-dimensional systems such as carbon nanotubes.²⁹ For the $\text{BN}(5,0)$ nanotube, the in-plane mode is softened and the frequency now is 1310 cm^{-1} . This effect can also occur in carbon nanotubes³⁰ because of the curvature effects.

In order to see more details about the Raman-active phonon modes, we try to find all the Raman active and IR active modes. Alon³¹ has shown that the rod group of the $\text{BN}(n,0)$ zigzag nanotubes is C_{2nv} . There are total $12n$ phonon modes for a $\text{BN}(n,0)$ nanotube. Four of them, which transform as $\Gamma_v = A_1 \oplus E_1$ and Γ_{R_z} , have vanishing frequencies at the Γ point. Two of the four modes are degenerate which can be seen from Fig. 5. The modes that transform according $\Gamma_t = A_1 \oplus E_1 \oplus E_2$ and/or Γ_v are Raman and/or IR active, respectively:

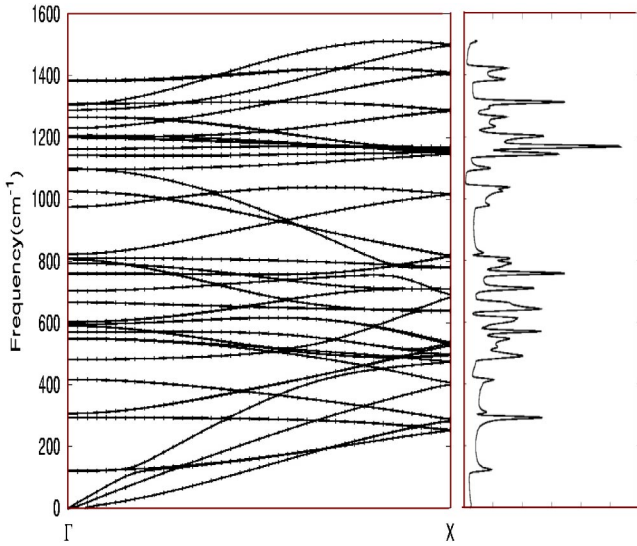


FIG. 5. Phonon band structure and density of states of the BN(5,0) nanotube.

$$\Gamma_{Raman}^{zig} = 3A_1 \oplus 5E_1 \oplus 6E_2,$$

$$\Gamma_{IR}^{zig} = 3A_1 \oplus 5E_1.$$

All IR active phonon modes are Raman active. We show the calculated frequencies of the Raman-active modes of several zigzag nanotubes in Fig. 6 and Ref. 32.

For BN nanotubes, the RBM is both Raman and IR active. Since the Raman spectrum is mainly related to the Γ phonon, we can calculate the phonon frequency of this mode efficiently by using only one unit cell in the force constant calculation. We use this method to calculate the RBM for six kinds of zigzag nanotubes: BN(5,0), BN(6,0), BN(7,0), BN(8,0), BN(10,0), BN(12,0), and two kinds of armchair nanotubes: BN(4,4) and BN(5,5). Figure 7 shows the calculated results. From this figure, we find that the frequency of the RBM decreases as the radius of the nanotube increases.

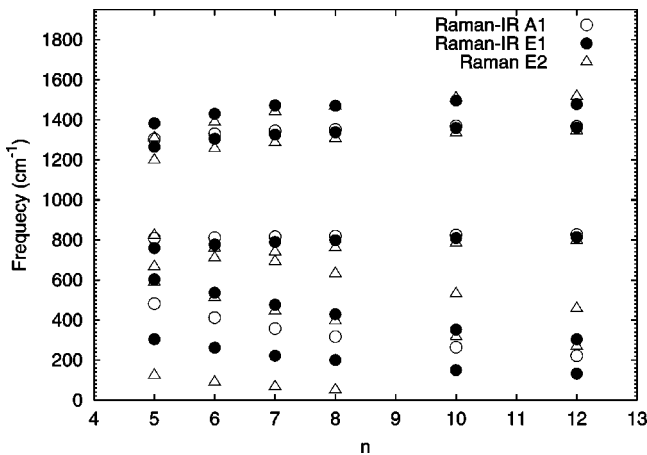


FIG. 6. Frequencies (cm^{-1}) of Raman-active modes of BN($n,0$) nanotubes ($n=5-8, 10$ and 12). For (10,0) and (12,0) nanotubes, the frequency of the lowest E_2 mode is close to zero, and is not plotted in the figure for clarity.

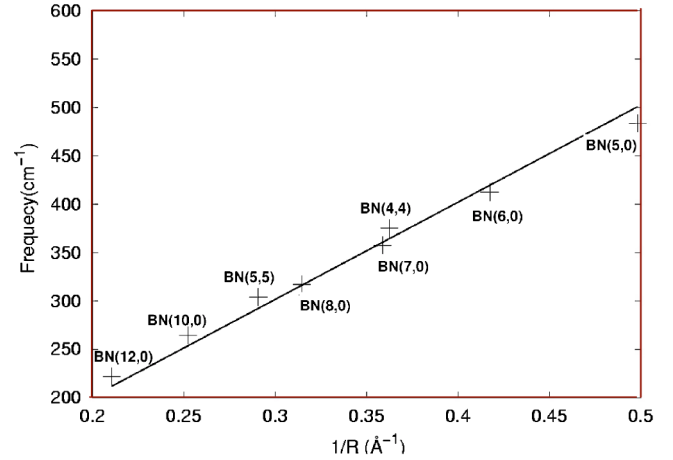


FIG. 7. Frequencies of the RBM of BN nanotubes. The radius refers to that of an unrelaxed BN nanotube.

We fit the results using the formula $\nu = A/R$ where R is the radius of the nanotube and $A = 1005 \text{ cm}^{-1} \text{ \AA}$. One can see from the figure the fitting is a straight line. The deviation from the linear fit is due to the two cylinders in the BN nanotubes. If all atoms lie in the same cylinder the frequency of the RBM will inversely proportional to the radius of the tubes. Because the distance of the two cylinders is smaller for large diameter nanotubes than that for small diameter nanotubes, we expect the fit will be better if we fit the results of the larger BN nanotubes. In fact, the BN nanotubes observed in experiments are larger than the ones studied here. Our obtained A value is a little smaller than that of carbon nanotubes.^{30,33} We expect the fitting formula will be useful for determining the radius of a BN nanotube from Raman spectra in experiments.

IV. SUMMARY

We have performed a first-principles study on the structural, electronic, and vibrational properties of small BN single-walled nanotubes. A growth mechanism is proposed as an explanation why zigzag nanotubes dominate in the products of BN nanotubes. The smallest stable BN nanotube is shown to be the BN(5,0) zigzag nanotube. We find that for small zigzag nanotubes the energy gap decreases rapidly with the decrease of radius, while armchair nanotubes almost have a constant energy gap. We have calculated the phonon dispersions of BN nanotubes and found the frequency of the RBM is inversely proportional to the nanotube radius.

ACKNOWLEDGMENT

This work was partially supported by the National Project for the Development of Key Fundamental Sciences in China (G1999075305, G2001CB3095), by the National Natural Science Foundation of China (50121202, 20025309, 10074058), by the Foundation of Ministry of Education of China, and by the Foundation of the Chinese Academy of Science.

- *Corresponding author. Email address: jlyang@ustc.edu.cn
- ¹Angel Rubio, Jennifer L. Corkill, and Marvin L. Cohen, Phys. Rev. B **49**, 5081 (1994).
- ²N.G. Chopra, R.J. Luyken, K. Cherrey, V.H. Crespi, M.L. Cohen, S.G. Louie, and A. Zettl, Science **269**, 966 (1995).
- ³X. Blase, A. Rubio, S.G. Louie, and M.L. Cohen, Europhys. Lett. **28**, 335 (1994).
- ⁴D. Golberg and Y. Bando, Appl. Phys. Lett. **79**, 415 (2001).
- ⁵M. Terauchi, M. Tanaka, K. Suzuki, A. Ogino, and K. Kimura, Chem. Phys. Lett. **324**, 359 (2000).
- ⁶X. Blase, A. De Vita, J.-C. Charlier, and R. Car, Phys. Rev. Lett. **80**, 1666 (1998).
- ⁷Madhu Menon and Deepak Srivastava, Chem. Phys. Lett. **307**, 407 (1999).
- ⁸Lu-Chang Qin, Xinluo Zhao, Kaori Hirahara, Yoshiyuki Miyamoto, Yoshinori Ando, and Sumio Iijima, Nature (London) **408**, 50 (2000); N. Wang, Z.K. Tang, G.D. Li, and J.S. Chen, *ibid.* **408**, 50 (2000).
- ⁹I. Cabria, J.W. Mintmire, and C.T. White, Int. J. Quantum Chem. **91**, 51 (2003).
- ¹⁰R.A. Jishi, L. Venkataraman, M.S. Dresselhaus, and G. Dresselhaus, Chem. Phys. Lett. **209**, 77 (1993).
- ¹¹A.M. Rao, E. Richter, S. Bandow, B. Chase, P.C. Eklund, K.A. Williams, S. Fang, K.R. Subbaswamy, M. Menon, A. Thess, R.E. Smalley, G. Dresselhaus, and M.S. Dresselhaus, Science **275**, 187 (1997).
- ¹²D. Sánchez-Portal and E. Hernández, Phys. Rev. B **66**, 235415 (2002).
- ¹³G. Kresse and J. Hafner, J. Phys.: Condens. Matter **6**, 8245 (1994).
- ¹⁴G. Kresse and J. Hafner, Phys. Rev. B **49**, 14251 (1994).
- ¹⁵G. Kresse and J. Hafner, Phys. Rev. B **47**, R558 (1993).
- ¹⁶G. Kresse and J. Furthmüller, Comput. Mater. Sci. **6**, 15 (1996); Phys. Rev. B **54**, 11169 (1996).
- ¹⁷D. Vanderbilt, Phys. Rev. B **41**, 7892 (1990).
- ¹⁸P. Hohenberg and W. Kohn, Phys. Rev. **136**, B864 (1964).
- ¹⁹W. Kohn and L.J. Sham, Phys. Rev. **140**, A1133 (1965).
- ²⁰J.P. Perdew and A. Zunger, Phys. Rev. B **23**, 5048 (1981).
- ²¹D.M. Ceperley and B.J. Alder, Phys. Rev. Lett. **45**, 566 (1980).
- ²²Konstantin N. Kudin, Gustavo E. Scuseria, and Boris I. Yakobson, Phys. Rev. B **64**, 235406 (2001).
- ²³E. Hernández, C. Goze, P. Bernier, and A. Rubio, Phys. Rev. Lett. **80**, 4502 (1998).
- ²⁴E. Hernández, C. Goze, P. Bernier, and A. Rubio, Appl. Phys. A: Mater. Sci. Proc. **68**, 287 (1999).
- ²⁵W. Frank, C. Elsässer, and M. Fähnle, Phys. Rev. Lett. **74**, 1791 (1995).
- ²⁶R.J. Nemanich, S.A. Solin, and R.M. Martin, Phys. Rev. B **23**, 6348 (1981).
- ²⁷Nobuko Ohba, Kazutoshi Miwa, Naoyuki Nagasako, and Atsuo Fukumoto, Phys. Rev. B **63**, 115207 (2001).
- ²⁸G. Kern, G. Kresse, and J. Hafner, Phys. Rev. B **59**, 8551 (1999).
- ²⁹M.S. Dresselhaus and P.C. Eklund, Adv. Phys. **49**, 705 (2000).
- ³⁰Daniel Sánchez-Portal, Emilio Artacho, José M. Soler, Angel Rubio, and Pablo Ordejón, Phys. Rev. B **59**, 12678 (1999).
- ³¹O.E. Alon, Phys. Rev. B **64**, 153408 (2001).
- ³²See EPAPS Document No. E-PRBMDO-68-019327 for a report on the vibrational frequencies of $BN(n,0)$ ($n=5-8,10,12$) single-wall nanotubes at γ . A direct link to this document may be found in the online article's HTML reference section. The document may also be reached via the EPAPS homepage (<http://www.aip.org/pubservs/epaps.html>) or from <ftp.aip.org> in the directory /epaps/. See the EPAPS homepage for more information.
- ³³J. Kuřti, G. Kresse, and H. Kuzmany, Phys. Rev. B **58**, 8889 (1999).